BIOCHEMISTRY
including biophysical chemistry & molecular biology

Article

pubs.acs.org/biochemistry

A Protein Arginine *N*-Methyltransferase 1 (PRMT1) and 2 Heteromeric Interaction Increases PRMT1 Enzymatic Activity

Magnolia L. Pak, Ted M. Lakowski, Dylan Thomas, Mynol I. Vhuiyan, Kristina Hüsecken, and Adam Frankel*

Faculty of Pharmaceutical Sciences, The University of British Columbia, Vancouver, British Columbia, Canada

Supporting Information

ABSTRACT: Protein arginine *N*-methyltransferases (PRMTs) act in signaling pathways and gene expression by methylating arginine residues within target proteins. PRMT1 is responsible for most cellular arginine methylation activity and can work independently or in collaboration with other PRMTs. In this study, we demonstrate a direct interaction between PRMT1 and PRMT2 using co-immunoprecipitation, bimolecular fluorescence complementation, and enzymatic assays. As a result of this interaction, PRMT2 stimulated PRMT1 activity, affecting its apparent V_{max} and K_M values in vitro and increasing the production of methylarginines in cells. Active site mutations and regional deletions from PRMT1 and -2 were also investigated, which demonstrated that complex formation required full-length, active PRMT1. Although the inhibition of methylation by adenosine dialdehyde prevented the interaction between PRMT1 and -2, it did not prevent the interaction between PRMT1 and a truncation mutant of PRMT2 lacking its Src homology 3 (SH3) domain. This result suggests that the SH3 domain may mediate an interaction between PRMT1 and -2 in a methylation-dependent fashion. On the basis of our findings, we propose that PRMT1 serves as the major methyltransferase in cells by forming higher-order oligomers with itself, PRMT2, and possibly other PRMTs.

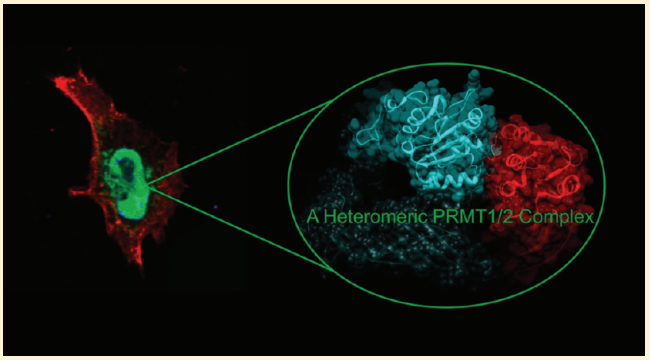

Protein arginine *N*-methyltransferases (PRMTs) methylate arginine residues within proteins by transferring methyl groups from *S*-adenosyl-L-methionine (AdoMet) to the terminal guanidino nitrogens of arginine residues, a post-translational modification that in part controls chromatin organization and cell growth.[1] Nine conserved members of the PRMT family have been reported to date. Except for PRMT9(4q31) in which activity has yet to be reported,[2] PRMT1,[3] PRMT2,[4] PRMT3,[5] coactivator-associated arginine methyltransferase 1 (CARM1/PRMT4),[6,7] PRMT6,[8] and PRMT8[9] all form ω-N^G-monomethylarginine (MMA or NMMA) and asymmetric ω-N^G,N^G-dimethylarginine (aDMA). PRMT5 forms MMA and symmetric ω-N^G,N'^G-dimethylarginine (sDMA),[10] and PRMT7 forms MMA and possibly sDMA.[11]

PRMT1 is the predominant arginine methyltransferase in human cells responsible for at least 85% of all arginine methylation activity,[12,13] targeting an array of different proteins, including nuclear receptors (NRs) such as hepatocyte nuclear receptor 4 (HNF4)[14] and estrogen receptor α (ERα),[15] chromatin-associated proteins such as histone H4 and H2A,[6,16,17] and RNA-binding proteins such as heterogeneous nuclear ribonucleoproteins (hnRNPs).[12,18−20] Studies have demonstrated that PRMT1 may collaborate with other PRMTs in specific cellular pathways. For example, PRMT1 and CARM1 have been shown to activate gene transcription synergistically.[21−24] Additionally, PRMT1 and -6 have been shown to work together in the base excision repair pathway by methylating DNA polymerase β in vivo in response to DNA damage.[25,26] It has been also demonstrated that PRMTs can exist within the same protein complexes as shown by co-immunoprecipitation.[9,27]

Structural studies of PRMT1,[28] its yeast homologue Rmt1p/Hmt1p,[29] PRMT3,[30] and CARM1[31,32] have suggested that PRMTs function as canonical homodimers in which a dimerization arm (helix−turn−helix motif) from one subunit makes reciprocal contact with the other subunit in the AdoMet-binding domain to form a ring structure with 2-fold symmetry. As evidence of these interactions, endogenous PRMTs have been co-immunoprecipitated by their ectopically expressed and tagged PRMT counterparts in cells.[9,33,34] Indeed, mutagenesis studies on rat PRMT1 and Rmt1p have demonstrated that their dimerization arms are required to form homodimers and stabilize cofactor binding for methyltransferase activity.[28,29] Also, phosphorylation of Ser-229 within the arm of CARM1 prevents its homodimerization, resulting in compromised enzyme activity.[35]

Relative to PRMT1, less is known about PRMT2 activity and its cellular functions. PRMT2 was first identified because of its

Received: April 27, 2011
Revised: August 16, 2011
Published: August 18, 2011

similarity to PRMT1,[36,37] yet it is the only PRMT family member that bears an N-terminal Src homology 3 (SH3) domain. Similar to PRMT1, PRMT2 has also been shown to act as a coactivator of transcription in response to ligand-dependent activation of NRs.[38,39] The coactivator function of PRMT1 has been attributed to its methylation of H4R3 and several translation factors (reviewed in ref 1). Our recent demonstration that PRMT2 can selectively methylate the N-terminal tail of histone H4, albeit several orders of magnitude less in vitro than PRMT1, suggests that its coactivator function may be a direct result of this activity.[4]

In this study, we investigate the relationship between PRMT1 and -2. Because both enzymes share overlapping substrate specificity in vitro, we initiated a series of experiments to see whether PRMT2 would affect PRMT1 activity toward histone H4 or vice versa, and we observed a synergistic (i.e., nonadditive) increase in the level of substrate methylation. Assaying combinations of wild-type and catalytically inactive PRMTs indicated that both PRMT1 and -2 mutants increased PRMT1 activity. The interaction between PRMT1 and -2 was confirmed in vitro and in HeLa cells by co-immunoprecipitation, as well as by bimolecular fluorescence complementation (BiFC). The BiFC technique can demonstrate a direct interaction in cells between two proteins that, when bound, mediate the reassembly of a fluorescent protein from its N- and C-terminal fragments attached to each binding partner.[40,41] We analyzed combinations of wild-type and mutant PRMT1 and -2 to further investigate their interaction in cells and determined that binding required the dimerization arm and catalytic activity of PRMT1. In the presence of adenosine dialdehyde (AdOx), which globally inhibits methylation, the interaction between PRMT1 and -2 was compromised, yet deletion of the PRMT2 SH3 domain restored the interaction in AdOx-treated cells or when PRMT1 was inactive. Our results reveal that the SH3 domain regulates the interaction between PRMT1 and -2 in a methylation-dependent manner. Moreover, this work represents the first evidence of a direct interaction between two PRMTs that culminates in a change in activity for one of the enzymes.

EXPERIMENTAL PROCEDURES

DNA Constructs. All DNA primers used in this study are listed in Table S1 of the Supporting Information. The humanized rat *PRMT1* gene encoding PRMT1v1 (isoform 1)[42] was subcloned into pcDNA3.1(+)/Neo (Invitrogen) using *Bam*HI and *Xho*I restriction sites. The human *PRMT2* gene previously subcloned into pGEX-2T[4] was amplified via polymerase chain reaction (PCR) with primers as described in Table S1 of the Supporting Information, digested with *Bam*HI and *Xho*I, and subcloned into pcDNA3.1(+)/Neo. Mutually annealing primers generated DNA sequences flanked by *Nhe*I sites encoding the hemagglutinin (HA) (YPYDVPDYA) and c-Myc (EQKLISEEDL) tags. *Nhe*I-digested DNA fragments encoding the c-Myc tag were subcloned into pcDNA3.1(+)/Neo-PRMT1 to generate pcDNA3.1(+)/Neo-c-myc-PRMT1 that encodes an N-terminal c-Myc-tagged PRMT1 protein. *Nhe*I-digested DNA fragments encoding the HA tag were subcloned into pcDNA3.1(+)/Neo-PRMT2 to generate pcDNA3.1(+)/Neo-HA-PRMT2 that encodes an N-terminal HA-tagged PRMT2 protein. The gene for histone H4 in pET3 was a generous gift from K. Luger (Colorado State University, Fort Collins, CO).

BiFC constructs encoding either mCitrineN (amino acid residues 1−173 of mCitrine) fused to the N-terminus of a PRMT or mCitrineC (amino acid residues 174−239 of mCitrine) fused to the C-terminus of a PRMT each contained a short and flexible amino acid linker (GGGGS) separating the fluorescent protein fragment from the enzyme that was successfully used in another study.[43] To make BiFC constructs, PRMT genes were first cloned into the pET28a vector at *Nde*I and *Xho*I sites for mCitrineN constructs, and at *Bam*HI and *Xho*I sites for mCitrineC constructs. The mCitrineN PRMTs were then amplified via PCR with primers containing *Hin*dIII and *Xho*I sites, and the mCitrineC PRMTs were amplified with primers containing *Bam*HI and *Eco*RI sites. The amplicons were subcloned into pcDNA3.1(+)/Hygro and pcDNA3.1(+)/Neo, respectively. Control constructs pcDNA3.1(+)/Hygro-mCitrineN-Only and pcDNA3.1(+)/Neo-mCitrineC-Only were made by PCR with primers containing *Hin*dIII and *Bam*HI sites for mCitrineN, and an *Xho*I site for mCitrineC. The amplicons were subcloned into pcDNA3.1(+)/Hygro for mCitrineN-Only and pcDNA3.1(+)/Neo for mCitrineC-Only.

Primers used for mutagenesis are listed in Table S2 of the Supporting Information. Site-directed mutagenesis reactions were conducted using the QuikChange method (Agilent Technologies).

Protein Expression and Purification. GST-PRMT2, GST-E220Q (PRMT2), 6xHis-PRMT1, and 6xHis-E153Q (PRMT1) were expressed and purified using previously described methods.[4,42] Histone H4 and its R3K mutant were overexpressed in BL21 DE3 pLysS *Escherichia coli* cells (Agilent Technologies) according to previously described methods.[44] Histone H4 and its R3K mutant were purified from inclusion bodies by denaturation in 20 mM Tris (pH 8.0), 8.0 M guanidinium hydrochloride, and 4.0 mM DTT, followed by rapid dilution in 100 mM Tris (pH 8.0), 400 mM arginine, 2 mM EDTA, 1 mM PMSF, and 0.5 mM oxidized glutathione and 5.0 mM reduced glutathione (total dilution of ∼1:50). Histone H4 and its R3K mutant were further purified using a Zorbax 9 mm × 250 mm C8 semipreparative reverse phase high-performance liquid chromatography column using 0.1% TFA in water and 0.1% TFA in acetonitrile (5 to 95% gradient developed over 20 min). Enzyme concentrations were determined using a previously described method.[4] The concentrations of histone H4 and its R3K mutant were determined using UV spectroscopy (ε_{280} = 5120 M^{-1} cm^{-1}).

Tissue Culture. HeLa cells were cultured in Dulbecco's modified Eagle's medium (DMEM) (Sigma) supplemented with 5% fetal bovine serum (FBS) (Gibco) and 100 μg/mL Primocin (InvivoGen) at 37 °C in 5% CO_2. Approximately 0.1 × 10^6 HeLa cells were seeded in each well of a 24-well plate containing a 12 mm microscope cover glass (Fisher) coated with poly-D-lysine (Sigma) and grown in standard growth medium for 24 h prior to transfection. Immediately before transfection, the growth medium was replaced with Opti-MEM medium (Invitrogen). HeLa cells were transiently cotransfected with the desired BiFC constructs (0.4 μg of DNA each) using Lipofectamine 2000 (Invitrogen) per the manufacturer's instructions. The medium was replaced with DMEM supplemented with 5% FBS, but without antibiotic 7 h post-transfection. The transfected cells were cultured for an additional 18 h before they were fixed. To inhibit cellular methylation, HeLa cells were transfected in a growth medium supplemented with 20 μM periodate-oxidized adenosine (AdOx) (Sigma).

Confocal Microscopy. The cells were allowed to grow for 25 h after cotransfection with BiFC constructs and before fixation with a 4% paraformaldehyde solution in phosphate-buffered saline (PBS) (Gibco, catalog no. 10010). The cells were then stained with Alexa Fluor 594 phalloidin (Invitrogen) and 2-(4-carbamimidoylphenyl)-1*H*-indole-6-carboximidamide (DAPI) (Invitrogen). Representative cell images of BiFC combinations were examined using a FluoView FV10i confocal microscope (Olympus), which provided an initial scan at 10× magnification to aid in identifying the fluorescence signal in all cells. High-resolution cell images were then captured with an oil lens at 60× magnification and subsequently processed with ImageJ (NIH image). Because of the strong background signal caused by the PRMT1E153Q-mCitrineC construct (Figure S1 of the Supporting Information), the laser input used for generating images of cells cotransfected with the PRMT1E153Q-mCitrineC construct was reduced by half to 7.2%. Otherwise, all images for BiFC were obtained with the same aperture (1×), sensitivity (49.6%), and laser input (14.1%) settings and processed without brightness and contrast adjustment.

Immunoprecipitation and Western Blotting. For immunoprecipitation of proteins from cells, 8×10^6 HeLa cells cultivated in a 100 mm dish for 24 h were transfected with 24 μg of DNA using Lipofectamine 2000 (Invitrogen) according to the manufacturer's protocol. To inhibit cellular methylation, HeLa cells were transfected in a growth medium supplemented with 20 μM AdOx.

After transfection, cells were harvested and lysed in 250 μL of hypotonic lysis buffer [20 mM HEPES-KOH (pH 7.4), 2 mM $MgCl_2$, 0.2 mM EGTA, 10% glycerol, and 1× protease inhibitor cocktail (Roche catalog no. 04693132001)] by repeated freezing and thawing. The NaCl concentration was then adjusted to 400 mM. The lysed cells were incubated on ice for 5 min and centrifuged at 14000 rpm at 4 °C for 15 min in an Eppendorf centrifuge (5417 R). Cell lysate (500 μg of protein) was aliquoted and the buffer adjusted to 50 mM HEPES-KOH and 150 mM NaCl. Aliquoted cell lysate was then supplemented with 2.0 μg of monoclonal anti-HA antibody (HA-7, Sigma), monoclonal anti-c-Myc antibody (9E10, Sigma), or mouse IgG (15381, Sigma), and the volume was adjusted to 500 μL with co-IP buffer [50 mM HEPES-KOH (pH 7.4), 150 mM NaCl, and 1× protease inhibitor cocktail]. The protein/antibody mixtures were incubated at 4 °C for 4 h with rotation. The cell lysate/antibody mixture was added to 50 μL of prewashed protein G-Sepharose (Invitrogen) and was rotated at 4 °C for 16 h. Subsequently, the resin was washed thoroughly with 0.05% Tween 20 in PBS five times before the bound proteins were eluted in sodium dodecyl sulfate–polyacrylamide gel electrophoresis (SDS–PAGE) sample buffer.

For in vitro immunoprecipitation, purified recombinant enzymes were preincubated at 37 °C for 1 h in 10 μL of methylation buffer (see below) without DTT, followed by the addition of 2.0 μg of anti-PRMT2 antibody (PRMT2–340) (Abcam) or 2.0 μg of mouse IgG (15381) (Sigma), and the volume was adjusted to 500 μL with co-IP buffer [50 mM HEPES-KOH (pH 7.4), 150 mM NaCl, and 1× protease inhibitor cocktail]. The protein/antibody mixtures were incubated at 4 °C for 4 h with rotation before being combined with 50 μL of prewashed protein G-Sepharose (Invitrogen) and incubated with rotation overnight at 4 °C. The resin was washed with PBS six times before the bound proteins were eluted in SDS–PAGE sample buffer.

For Western blots, proteins were separated on 10% SDS–PAGE gels and transferred to nitrocellulose membranes. The membranes were blocked with a 5% TBS/milk solution at 37 °C for 2 h and blotted with monoclonal anti-c-Myc antibody (9E10) (Sigma), monoclonal anti-HA antibody (HA-7) (Sigma), monoclonal anti-PRMT1 antibody (PRMT1–171) (Sigma), or monoclonal anti-PRMT2 antibody (PRMT2–340) (Abcam) in a 3% TBST/milk solution at 4 °C for 16 h. Goat anti-mouse light chain horseradish peroxidase-conjugated secondary antibody (Millipore) or goat anti-mouse IgG-HRP (sc-2005) (Santa Cruz) and ECL Western blotting detection reagents (GE Healthcare) were used for protein visualization.

Methylation Assays. Purified PRMTs and mutants were preincubated at 37 °C for 1 h in methylation buffer [50 mM HEPES-KOH (pH 8.0), 10 mM NaCl, and 1 mM DTT] as previously described to equilibrate heteromeric complexes[4,42] before initiation of the methylation reaction with final concentrations of 10 μM histone H4 and 100 μM *S*-adenosyl-L-[*methyl*-^{14}C]methionine (Perkin-Elmer; 1.8056 Gbq mmol^{-1}; concentrated as described in ref 42). Either wild-type PRMT or mutant concentrations were fixed, and the other was increased to molar ratios of 0, 2, 4, 7, 11, 19, 30, and 50 with one noted exception (Figure 1C). The final concentration of glycerol was less than 2.5% so that enzyme activities were not affected.[4,42] Methylation proceeded at 37 °C for 1 h, where the level of PRMT1 was held constant, and 16 h,

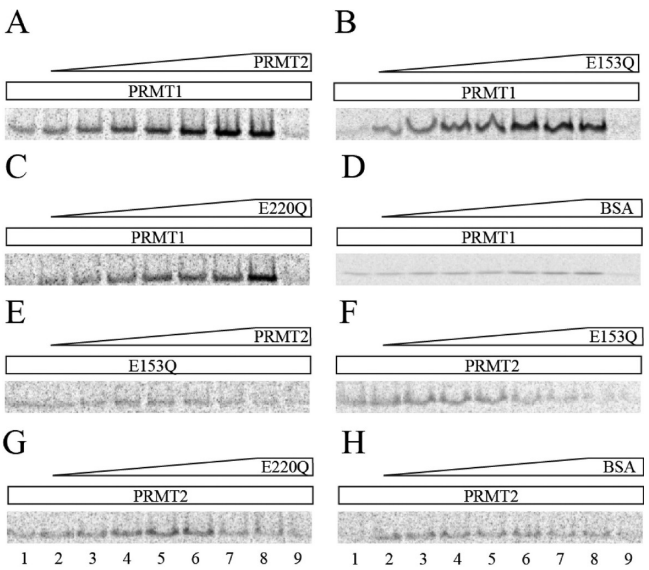

Figure 1. Synergistic methylation of histone H4 by PRMT1 and -2. Preincubations of enzymes without substrates were performed at 37 °C for 1 h in methylation buffer prior to initiation of 1 h methylation reactions. (A) Reaction mixtures included 100 nM PRMT1 alone (lane 1), 100 nM PRMT1 with 210–5000 nM PRMT2 (lanes 2–8), and 5000 nM PRMT2 alone (lane 9). Similar reactions were prepared with PRMT1 and (B) PRMT1 E153Q, (C) 100–2500 nM PRMT2 E220Q, and (D) BSA. (E) Samples were prepared as described for panel A except 100 nM PRMT1 E153Q was used in place of PRMT1. (F) Preincubations were performed as described for panel A with 400 nM PRMT2 alone (lane 1), 400 nM PRMT2 with 800–20000 nM PRMT1 E153Q (lanes 2–8), and 20000 nM PRMT1 E153Q alone (lane 9) prior to initiation of 16 h methylation reactions. Similar reaction mixtures were prepared with PRMT2 and (G) PRMT2 E220Q and (H) BSA. Coomassie-stained gels and full-size storage phosphor images are shown in Figure S4 of the Supporting Information.

where the level of PRMT2 was held constant, and stopped by a 10 min incubation at 90 °C. Samples were then dried in a vacuum centrifuge and reconstituted in SDS−PAGE sample dilution buffer with 6 M urea. Dissolved samples were separated on 15% Tricine gels and exposed to storage phosphor screens for 18 h before being imaged on a Typhoon 9400 instrument (GE Healthcare).

Enzyme Kinetics. Apparent enzymatic kinetic parameters were determined at a 25 nM:750 nM (1:30) ratio for PRMT1 with its E153Q mutant, and PRMT1 with the PRMT2 E220Q mutant. Reactions were preformed like the gel assays described above in methylation buffer with a 1 h preincubation of the enzymes at 37 °C in the absence of substrates to equilibrate heteromeric complexes. The 1:30 ratio was chosen because it is the minimum ratio that produces the maximum increase in PRMT1 activity observed in Figure 1, and the PRMT1 concentration falls within the linear range of the enzyme because a linear increase in the level of formation of methylated arginines with an enzyme concentration increasing from 6.25 to 100 nM was observed (Figure S2 of the Supporting Information). For both groups of enzymes, reactions to determine the apparent kinetic parameters with histone H4 were performed with a constant AdoMet concentration of 100 μM and varied histone H4 concentrations of 0, 0.25, 0.5, 1.0, 2.0, 5.0, 10, 20, 30, and 40 μM. Reactions to determine the apparent kinetic parameters for AdoMet were performed with a constant histone H4 concentration of 40 μM and varied AdoMet concentrations of 0, 0.25, 0.5, 1.0, 2.0, 5.0, 10, 20, 50, and 100 μM. Reactions were stopped by a 10 min incubation at 90 °C, and the dried samples were hydrolyzed with 6.0 M HCl at 110 °C for 24 h under vacuum.

An Agilent 1290 Infinity LC system was connected to a Waters UPLC BEH C18 column (2.1 mm × 100 mm) at a flow rate of 0.15 mL/min at 45 °C. The mobile phases of 0.1% aqueous formic acid and 0.05% TFA (A) and 0.1% formic acid, 0.05% TFA, and 30% methanol (B) were used in a linear gradient from 0 to 20% B over 2.3 min. Samples were analyzed on an AB SCIEX 5500 QTRAP tandem mass spectrometer using positive ion multiple-reaction monitoring in separate channels for MMA and aDMA. Parent and fragment ions used for quantitation corresponded to amino acids as follows: MMA, m/z 189 and 74; aDMA, m/z 203 and 46. The cone voltage was 30 V, and the collision energy was 20 eV for aDMA and 17 eV for MMA. Apparent enzymatic kinetic parameters were determined by fitting the data to the Michaelis−Menten equation using SigmaPlot 8 (SYSTAT). The k_{cat} values were calculated on the basis of the molecular weight of the active monomer.

Methylation in Cells. Approximately 8 × 10^6 HeLa cells cultivated in a 100 mm dish were transfected with mammalian expression vectors (24 μg of total DNA; 12 μg of each construct for cotransfections) using Lipofectamine 2000 (Invitrogen) following the manufacturer's protocol. After being transfected, cells were harvested and resuspended in 1.0 mL of 50 mM sodium phosphate (pH 7.5). Cells were lysed by four 10 s sonicator pulses (50% duty, setting 2) on ice and centrifuged at 18000*g* for 30 min at 4 °C. Total protein concentrations were determined using the Bradford protein assay (Bio-Rad).

For simultaneous quantification of MMA, aDMA, and sDMA using mass spectrometry, 100 μL aliquots (approximately 200 μg of protein) of cell lysates from transfected HeLa cells described above were mixed with an equal volume of acetone and dried in a vacuum centrifuge. Dried samples were hydrolyzed as described above and reconstituted in 300 μL of 10 mM NaH_2PO_4 (pH 5.0), and basic amino acids were purified using Oasis MCX solid phase extraction (SPE) cartridges (Waters) according to previously described methods.[45] Dried purified samples were reconstituted in 100 μL of 0.1% aqueous formic acid and 0.05% TFA. Simultaneous quantification of MMA, aDMA, sDMA, and histidine was achieved with a Waters Acquity chromatographic system using the column, mobile phases, and conditions described in Enzyme Kinetics. A Quatro Premier XE electrospray tandem mass spectrometer (Micromass MS Technologies) was operated in positive ion mode for multiple-reaction monitoring in separate channels for MMA, aDMA, sDMA, and histidine. Parent and fragment ions used for quantitation corresponded to amino acids as follows: MMA, m/z 189, and m/z 74 and 144; aDMA, m/z 203 and 46; sDMA, m/z 203 and 172; histidine, m/z 156 and 110. In all cases, the cone voltage was 30 V and the collision energy was 20 eV except for MMA (for which it was 17 eV).

Using the conditions described above, we were able to unambiguously differentiate aDMA and sDMA despite their similar retention times and the same parent ion mass. Even at concentrations used for standards, ≥5.0 μM aDMA was not spuriously detected as sDMA and vice versa (Figure S3 of the Supporting Information). Standards of MMA, aDMA, and sDMA (Sigma) were used to prepare standard curves for quantification. All derived concentrations for MMA, aDMA, and sDMA were normalized by the relative peak area for histidine to control for differences in total protein (values typically varied by <10%). Histidine was used for this purpose because it is a basic amino acid that is retained on SPE cartridges along with arginine derivatives (data not shown). All samples were prepared in quadruplicate, and total levels of MMA, aDMA, and sDMA derived from vector-only controls (average values of 0.73 ± 0.05, 8.2 ± 0.4, and 1.1 ± 0.05 μM, respectively) were subtracted from experimental values. HeLa cells untransfected and transfected with the vector-only controls differed by <10% in methylarginine content.

RESULTS

PRMT2 and Its Inactive Mutant Potentiate the Methylation Activity of PRMT1 in Vitro. In our previous work, the comparatively high activity of PRMT1 toward histone H4 contrasted to the approximately 600-fold lower activity of PRMT2 toward the same substrate.[4] We wanted to then test if these two enzymes could interact and thereby change their respective activities. In this study when we mixed both enzymes with substrates at stoichiometric concentrations, no change in histone H4 methylation occurred (data not shown). When a 2−50-fold excess of PRMT2 was preincubated for 1 h with PRMT1 prior to the addition of AdoMet and histone H4, an up to 6.7-fold increase in methylation activity was found at the highest enzyme ratio as measured by densitometry (Figure 1A). Importantly, to elicit the synergistic increase in methylation activity, PRMT1 and -2 were preincubated for 1 h without substrates in accordance with our previous studies on PRMT interactions.[42] These facts suggest that the effect was caused by a direct interaction between PRMT1 and -2.

We then wanted to determine which enzyme was activating which by first using catalytically inactive PRMT1 mutation E153Q[28] and the corresponding E220Q mutation in PRMT2 (Figure S5A of the Supporting Information). As shown in panels B and C of Figure 1, an increasing concentration of E153Q or E220Q with a constant concentration of PRMT1

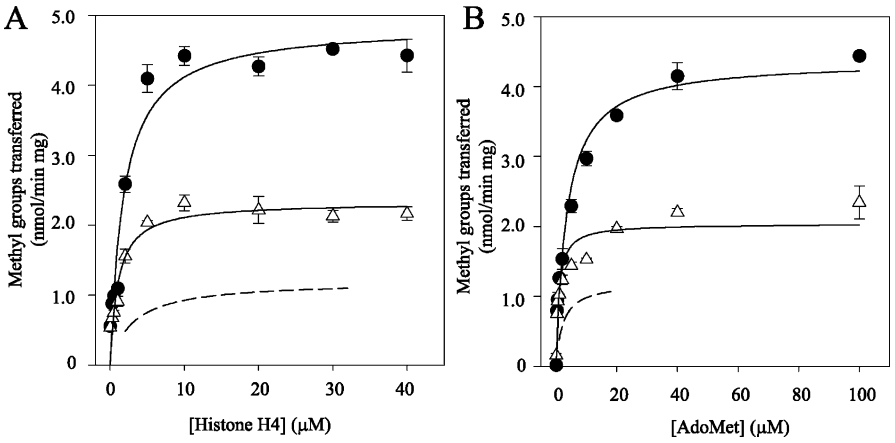

Figure 2. Synergistic methylation of histone H4 by PRMT1 with inactive PRMT1 and −2 mutants. The initial rate of enzymatic activity of PRMT1 with its E153Q mutant at a 25:750 ratio (●) and PRMT1 with the E220Q mutant of PRMT2 at a 25:750 ratio (△). (A) The concentration of AdoMet was held constant at 100 μM and that of histone H4 varied. (B) The concentration of histone H4 was held constant at 40 μM and that of AdoMet varied. Shown are means and standard deviations of two samples determined using UPLC MS/MS (Experimental Procedures). Total methylation was summed using the equation 2aDMA + MMA. For comparison, the initial rate of enzymatic activity of PRMT1 in the absence of other PRMTs (---) using data replotted from ref 4 is shown. In this case, the concentration of AdoMet was constant at 20 μM while that of histone H4 varied (A) and the concentration of histone H4 was constant at 32 μM while that of AdoMet varied (B).

demonstrated a maximum 15- or 8-fold increase in the level of histone H4 methylation, respectively. To show that the results from Figure 1A−C were not the result of nonspecific protein binding, the same amounts of bovine serum albumin (BSA) were preincubated with PRMT1, which showed in Figure 1D a comparatively modest increase (1.8-fold) in PRMT1 activity at the highest BSA concentration. These results imply that the increase in PRMT1 activity observed with PRMT2 (Figure 1A), as well as with the mutants of PRMT1 (Figure 1B) and PRMT2 (Figure 1C), was the result of specific protein−protein interactions. In contrast, increasing the level of wild-type PRMT2 with a constant concentration of E153Q did not result in any above-background methylation of histone H4 (Figure 1E). These results indicate that PRMT2, independent of its own activity, increased the activity of PRMT1. Moreover, the synergistic effect of E153Q on PRMT1 activity suggests that a higher-order oligomeric complex may be required for maximum PRMT1 activity.

To test for any change in PRMT2 activity in response to other PRMT subunits, a constant concentration of PRMT2 was incubated with increasing concentrations of E153Q (Figure 1F) and E220Q (Figure 1G). Increasing concentrations of E153Q and E220Q resulted in 1.4- and 2.1-fold increases in PRMT2 activity up to molar ratios of 11 and 19, respectively, before the activities decreased to background levels. A similar titration was performed with constant PRMT2 and increasing BSA concentrations, which produced no increase in PRMT2 activity (Figure 1H).

Because PRMT1 methylation of histone H4 at the Arg-3 position has already been well established,[16,17] and we have demonstrated PRMT2 activity toward histone H4 in vitro[4] (Figure S5 of the Supporting Information), we wanted to determine if PRMT2 affected where PRMT1 methylates histone H4. Wild-type histone H4 and its R3K mutant were used as substrates for preincubated PRMT1, PRMT2, and a mixture of both enzymes. In all cases in which the histone H4 R3K mutant was employed, the level of methylation was similar to the level of automethylation for the respective enzyme, whereas when wild-type histone H4 was used, the level of methylation was higher than the no-substrate control and histone H4 R3K substrate reactions (Figure S6 of the Supporting Information). The preincubated combination of PRMT1 and -2 produced the largest amount of arginine methylation formed on wild-type histone H4. These results confirmed that the major site of methylation on histone H4 in vitro is R3 for PRMT1 and -2 individually and together.

The effects of the interactions between PRMT1 and the inactive mutants of PRMT1 and PRMT2 on the enzyme kinetics of PRMT1 were determined by estimation of apparent enzyme kinetic parameters. We intentionally avoided estimations in which both enzymes were active because this scenario would be too complex to model and difficult to interpret. We note, however, that the potential for catalytically inactive enzyme to bind substrate could be a possible confounding variable in the estimation of the apparent K_M.

The initial rates of PRMT1 in the presence of E153Q or E220Q with a fixed concentration of AdoMet and variable histone H4 are plotted in Figure 2A, and the apparent kinetic parameters are listed in Table 1. For both enzyme combinations, the activity of PRMT1 was enhanced with respect to that of PRMT1 alone. When combined with E153Q the histone H4 V_{max} for PRMT1 was more than 4-fold greater than PRMT1 alone and the k_{cat} was more than 2.5-fold higher. Smaller increases in V_{max} and k_{cat} were also observed for PRMT1 with E220Q. This difference appears to be driven primarily by a doubling in the rate of formation of aDMA in the PRMT1/E153Q groups versus the PRMT1/E220Q groups (Figure S7 of the Supporting Information). PRMT1 with E153Q or E220Q resulted in a 2- or 4-fold reduction in K_M for histone H4, respectively, compared to that for PRMT1 alone. The changes in PRMT1 activity were also reflected in a 6- or 5-fold increase in the histone H4 specificity constant (k_{cat}/K_M) for PRMT1 with E153Q or E220Q, respectively.

The initial rate of PRMT1 in the presence of E153Q or E220Q with a fixed concentration of histone H4 and a variable level of AdoMet is plotted in Figure 2B, and the apparent kinetic parameters are listed in Table 1. As with histone H4, the AdoMet V_{max} and k_{cat} for PRMT1 with either mutant were increased with respect to those of PRMT1 alone. However, the AdoMet K_M for PRMT1 with E153Q resulted in a 3.5-fold

Table 1. Apparent Kinetic Parameters for PRMT1 with E153Q or E220Q[a]

enzyme	substrate	K_M (μM)	V_{max} (nmol min^{-1} mg^{-1})	k_{cat} ($\times 10^{-3}$ s^{-1})	k_{cat}/K_M (M^{-1} s^{-1})
PRMT1/E153Q	AdoMet	3.5 (0.4)	4.4 (0.02)	3.2 (0.02)	910 (100)
PRMT1/E153Q	histone H4	1.8 (0.1)	4.9 (0.1)	3.6 (0.1)	2000 (40)
PRMT1/E220Q	AdoMet	0.9 (0.04)	2.0 (0.07)	1.5 (0.05)	1700 (10)
PRMT1/E220Q	histone H4	1.0 (0.01)	2.3 (0.1)	1.7 (0.08)	1700 (70)
PRMT1[b]	AdoMet	1.0 (0.1)	1.2 (0.2)	1.3 (0.2)	1400 (20)
PRMT1[b]	histone H4	4.2 (0.2)	1.2 (0.2)	1.4 (0.2)	320 (40)

[a]The apparent kinetic parameters were determined by measuring the initial rate of enzymatic activity of PRMT1 with its E153Q mutant at a 25:750 ratio, and PRMT1 with the E220Q mutant of PRMT2 at a 25:750 ratio, and were derived from the total amount of methylation. The values are listed as means (standard deviation) of two measurements. [b]Values derived from ref 4.

increase compared to that of PRMT1 alone, a change not observed for PRMT1 with E220Q. The addition of mutants to PRMT1 resulted in an AdoMet k_{cat}/K_M for PRMT1 with E153Q that was 0.33-fold lower than that of PRMT1 alone, while the AdoMet k_{cat}/K_M for PRMT1 with E220Q was 1.25-fold higher. Altogether, the results of these kinetic experiments suggest that various oligomeric combinations of PRMT1 with mutants of PRMT1 and PRMT2 exhibit different enzymatic activities and substrate specificities.

Ectopic Expression of PRMT1 and -2 Synergistically Increases Protein Arginine Methylation in Cells. To test whether PRMT2 and its inactive mutant can also potentiate the methylation activity of PRMT1 in a cellular environment, we transiently transfected HeLa cells with wild-type and mutant PRMT1 and -2 individually and in combination. Cell lysates were hydrolyzed and analyzed for their MMA, aDMA, and sDMA content via tandem mass spectrometry. As shown in Figure 3, the concentrations of methylarginines are displayed

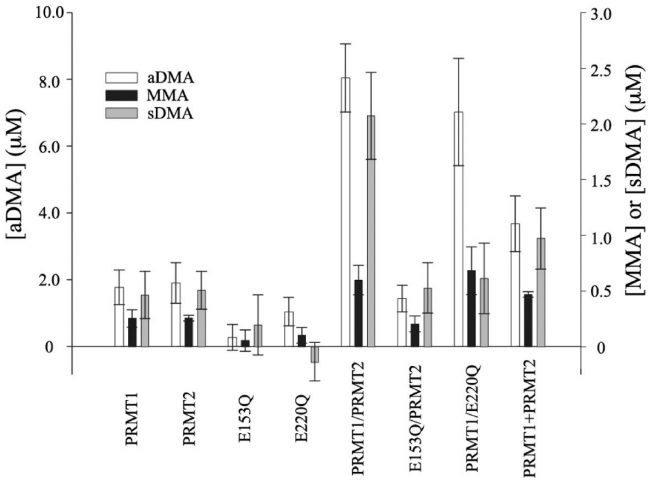

Figure 3. PRMT1- and PRMT2-dependent increases in cellular Protein Arginine Methylation. Cell lysates from transfected HeLa cells were prepared for tandem mass spectrometry to quantify MMA, aDMA, and sDMA derived from cellular protein. Concentrations are reported after background subtraction from the vector-only control. The set of bars on the far right shows the sum of PRMT1 and -2 groups to reveal the synergistic methylation with PRMT1 and -2 and PRMT1/E220Q groups. Values represent the mean and standard deviation (n = 4). Because of large differences in analyte concentrations, the right y-axis is scaled for MMA and sDMA and the left y-axis for aDMA.

after background subtraction from vector-only controls. The ectopic expression of PRMT1 or -2 alone resulted in small increases in the levels of MMA and aDMA as a likely consequence of increased PRMT levels. Interestingly, the levels of sDMA also increased, which neither PRMT1 nor PRMT2 is expected to make. HeLa cells transfected with E153Q or E220Q produced similar amounts of methylarginines to vector-only controls. On the other hand, HeLa cells cotransfected with PRMT1 and PRMT2 or its E220Q mutant produced a synergistic increase in the level of aDMA and to a lesser extent MMA, results consistent with the observed increases in the level of methylation in vitro (Figure 1). Surprisingly, a similar synergistic increase in the level of formation of sDMA was also observed with cells cotransfected with PRMT1 and -2, but not with PRMT1 and E220Q or E153Q and PRMT2, implying that the combination of enzymes can increase the level of formation of sDMA when PRMT1 is active. These dramatic increases in the number of protein methylarginines detected by tandem mass spectrometry did not closely match differences between samples observed by Western blotting for aDMA in proteins (Figure S8 of the Supporting Information), so we were unable to pinpoint which substrates other than histone H4 were more methylated in response to ectopically expressed PRMT1 and -2 as compared to controls.

PRMT1 and -2 Interact in Vitro and in Cells. To confirm a direct interaction between PRMT1 and -2 implied by in vitro experiments described above, we performed in vitro co-immunoprecipitation experiments between the wild type and inactive mutants of PRMT1 and PRMT2. Regardless of whether wild-type or mutant enzymes were used, the immunoprecipitated proteins were enriched above the level of the IgG controls (Figure 4A). These results demonstrate that PRMT1 and PRMT2 can interact directly in the absence of both AdoMet and protein substrates. Moreover, the in vitro interaction between these enzymes was not dependent upon their enzymatic activities based on binding results with E153Q and E220Q mutants.

We then tested if PRMT1 and -2 interact in cells. We expressed HA-tagged PRMT1, E153Q, PRMT2, and E220Q in HeLa cells, immunoprecipitated the HA-tagged proteins, and performed Western blots for endogenous PRMTs. Consistent with the in vitro co-immunoprecipitation results, endogenous PRMT2 was co-immunoprecipitated with HA-tagged PRMT1 or E153Q (Figure 4B). Similarly, endogenous PRMT1 was co-immunoprecipitated with HA-tagged PRMT2 or E220Q (Figure 4C). These results suggest that PRMT1 and -2 interact in cells, as well. We have also noticed that endogenous PRMT2 was also co-immunoprecipitated with HA-tagged PRMT2 or E220Q (Figure S9A of the Supporting Information).

Visualization of PRMT Interactions in Cells. To capture potential interactions between PRMTs in cells, we have employed a technique that was initially pioneered by Regan and co-workers, who showed that the stable reconstitution of green fluorescent protein (GFP) from its N- and C-terminal fragments (i.e., separate polypeptides) was mediated only by

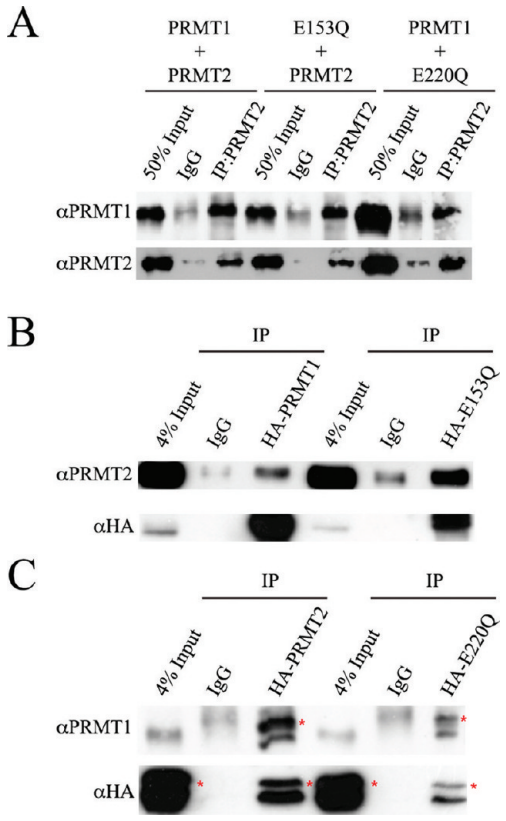

Figure 4. PRMT1 and -2 co-immunoprecipitate in vitro and in cells. (A) Indicated combinations of PRMTs (0.5 μg each) were preincubated at 37 °C for 1 h in methylation buffer and subsequently immunoprecipitated with anti-PRMT2 antibody or with mouse IgG (negative control). Immunoprecipitates were immunoblotted with either anti-PRMT1 (top) or anti-PRMT2 (bottom) antibodies. (B) HA-PRMT1 and HA-E153Q were expressed in HeLa cells, and the cell lysate was immunoprecipitated with anti-HA antibody or with mouse IgG (negative control). Immunoprecipitates were immunoblotted with anti-PRMT2 (top) or anti-HA (bottom) antibodies. (C) HA-PRMT2 or HA-E220Q was expressed in HeLa cells, and the cell lysate was immunoprecipitated with anti-HA antibody or with mouse IgG (negative control). Immunoprecipitates were immunoblotted with anti-PRMT1 (top) or anti-HA (bottom) antibodies. Nonspecific bands are labeled with red asterisks.

interacting proteins attached to each fragment of GFP.[40,46] Kerppola and co-workers adapted this concept to fluorescence microscopy in mammalian cells, which is termed bimolecular fluorescence complementation (BiFC).[41] BiFC has since emerged as a powerful tool for capturing images of specific and even transient protein−protein interactions in cells.[47−50] An important feature of this technique is the fact that requisite post-translational modifications, subcellular localization, and association with other proteins that may facilitate specific protein binding can occur within the native environment provided by the mammalian host cell. We designed expression vectors that produce N- and C-terminal fragments of the fluorescent protein mCitrine[51] fused to wild-type and mutant PRMTs to test for reconstituted fluorescence as evidence of PRMT−PRMT interactions in cells. Negative control vectors were devoid of *PRMT* genes.

Using BiFC in HeLa cells that have been transiently cotransfected with mCitrineN-PRMT1 and PRMT1-mCitrineC (Figure 5A), we observed a robust fluorescence signal via confocal microscopy that provides direct evidence that PRMT1 has the capacity to self-associate in the nucleus of cells (Figure 5Bi). When PRMT2 was tested in different BiFC combinations, only coexpression of mCitrineN-PRMT2 and PRMT1-mCitrineC resulted in a fluorescence signal (Figure 5Biv), revealing a potential orientation-specific interaction between PRMT1 and -2. Although detected in co-immunoprecipitation experiments (Figure S9A of the Supporting Information), we did not observe PRMT2 homodimerization with BiFC (Figure 5Bv). This result may be a function of the inability of PRMT2-mCitrineC to form any BiFC interactions despite its successful expression in cells (data not shown). Additionally, the mCitrineN-PRMT1/PRMT2-mCitrineC pair did not produce any above-background signal either (Figure 5Bii), which may have been caused by insufficient expression of mCitrineN-PRMT1 (Figure S10 of the Supporting Information), although this scenario is unlikely because the fusion protein was capable of participating in other BiFC complexes. To demonstrate that BiFC was selective for PRMT−PRMT interactions, HeLa cells were cotransfected with mCitrineN-Only or mCitrineC-Only in combination with mCitrine fragments attached to PRMTs, and these cells exhibited low-level background fluorescence (Figure 5Biii,vi−ix). Therefore, fluorescence signals generated by PRMT1 and PRMT1−PRMT2 complexes represent specific protein−protein interactions in HeLa cells.

PRMT Domains Required for Formation of the BiFC Complex in Cells. Having established an interaction between human PRMT1 and -2, we sought to determine the structural features important for their binding. Although no structure of the PRMT2 catalytic core has been determined, its 64% sequence similarity to PRMT1 within the arm region (PRMT1, residues 188−222; PRMT2, residues 256−294) evokes the possibility that PRMT2 may exhibit a similar binding modality. To test this hypothesis, we cotransfected BiFC constructs of PRMT1 and -2 lacking their respective dimerization arms in combination with wild-type enzymes (Figure 6A). Consistent with results from a previous study that showed the requirement of the dimerization arm for PRMT1 oligomerization,[28] the PRMT1Δ188−222 mutant did not yield any fluorescence indicative of a PRMT1 complex (Figure 6Bi,ii) or a PRMT1−PRMT2 complex (Figure 6Bv). These negative BiFC results were not due to unsuccessful cotransfection of HeLa cells because these proteins were detected by Western blot analysis (Figure S10 of the Supporting Information). We did detect some fluorescence signal in cells expressing the mCitrineN-PRMT2Δ256−294/PRMT1-mCitrineC pair; however, co-immunoprecipitation results between HA-PRMT2Δ256−294 and endogenous PRMT1 did not show any interaction (Figure S9B of the Supporting Information), making our results pertaining to the dimerization arm of PRMT2 inconclusive.

We explored the possibility that the SH3 domain of PRMT2 may mediate complex formation. Clarke, Bedford, and co-workers had previously shown that the PRMT2 SH3 domain could interact with the N-terminus of PRMT8, which contains two stretches of proline-rich amino acid sequences.[52] Even though PRMT1 does not contain any polyproline sequences, perhaps the SH3 domain of PRMT2 could potentially mediate an interaction with PRMT1. Therefore, the BiFC construct from which the PRMT2 SH3 domain was deleted (ΔSH3PRMT2) was cotransfected with PRMT1-mCitrineC to explore this possibility. As shown in Figure 6Bvii, even without its SH3 domain PRMT2 was still able to form the BiFC complex with PRMT1. This result indicates that the SH3

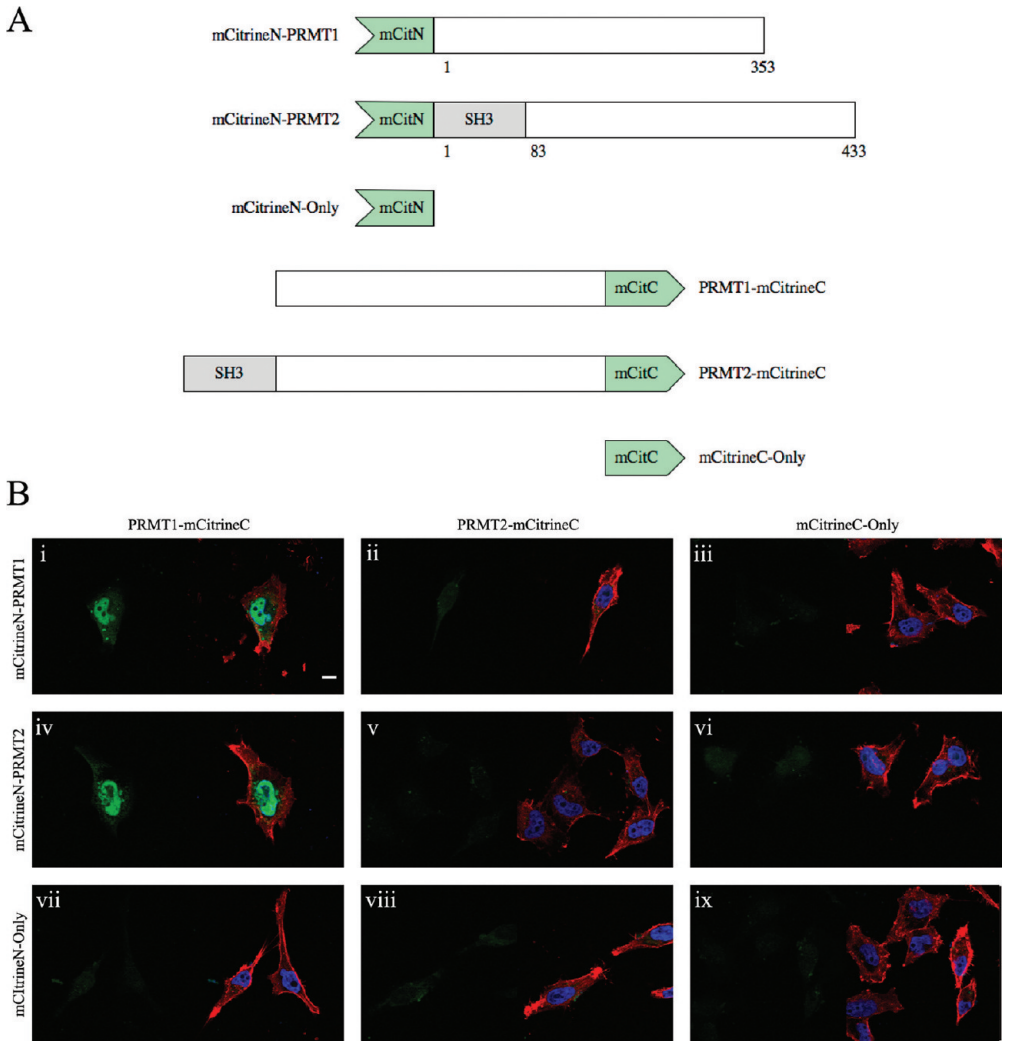

Figure 5. Visualization of PRMT1 and -2 interactions via BiFC. (A) Illustration of BiFC fusion proteins used in these experiments. (B) HeLa cells were cotransfected with the two constructs indicated in the columns and rows (representative images are shown). The left image of each row shows the formation of a BiFC complex. The right image of each row shows an overlay of BiFC (green), DAPI (blue), and fluorescence-labeled phalloidin (red). The scale bar is 10 μm.

domain was not directly responsible for the interaction between PRMT1 and -2.

PRMT Activity Requirements for Formation of the BiFC Complex in Cells. To further explore conditions that affect PRMT−PRMT interactions in HeLa cells, BiFC constructs of E153Q and E220Q mutants were employed (Figure 7A). Cells expressing combinations of wild-type and mutant PRMT1 showed BiFC signals (Figure 7Bi and Figure S9i,ii of the Supporting Information), indicating that enzyme activity from one or both subunits was not a requirement for self-association. When E153Q was tested with PRMT2, no above-background fluorescence was observed (Figure 7Bii), thus directly implicating PRMT1 activity as a requirement for the formation of the BiFC complex between PRMT1 and -2 in cells. This result contrasts with the co-immunoprecipitation results for E153Q and PRMT2 for which an interaction was detected (Figure 4), revealing that PRMT1 inactivity from the E153Q mutation prevented reassembly of fluorescent protein fragments. Interestingly, when the combination of E153Q and ΔSH3PRMT2 was tested for BiFC, a predominantly nuclear fluorescence signal was observed (Figure 7Biii). The results of these pairings imply that the BiFC complex between PRMT1 and -2 requires PRMT1 activity, but not when the SH3 domain of PRMT2 is removed.

The E220Q mutant behaved like wild-type PRMT2 in the BiFC assay with wild-type PRMT1 (Figure S11iii of the Supporting Information) and E153Q (Figure 7Biv). These results indicate that PRMT2 activity is not required for its interaction with PRMT1 and does not contribute to formation of the PRMT1−PRMT2 complex.

Because the PRMT1 E153Q mutation prevented its interaction with full-length PRMT2, we wanted to see if small-molecule inhibition of methyltransferase activity could also affect the interaction between PRMT1 and -2. Thus, we tested these BiFC combinations in the presence of 20 μM AdOx, which increases the intracellular levels of *S*-adenosyl-L-homocysteine to globally inhibit the methylation of arginine residues and other AdoMet-dependent enzyme substrates.[12,53] HeLa cells grown in AdOx did not appear to affect BiFC complex formation for PRMT1 constructs (Figure 7Bv), thus providing further evidence that PRMT1 activity is not essential for its self-association. When PRMT1 was tested for BiFC with PRMT2 in AdOx-treated cells, however, little if any fluorescence was observed (Figure 7Bvi,viii). This result is

dx.doi.org/10.1021/bi200644c | *Biochemistry* 2011, 50, 8226–8240

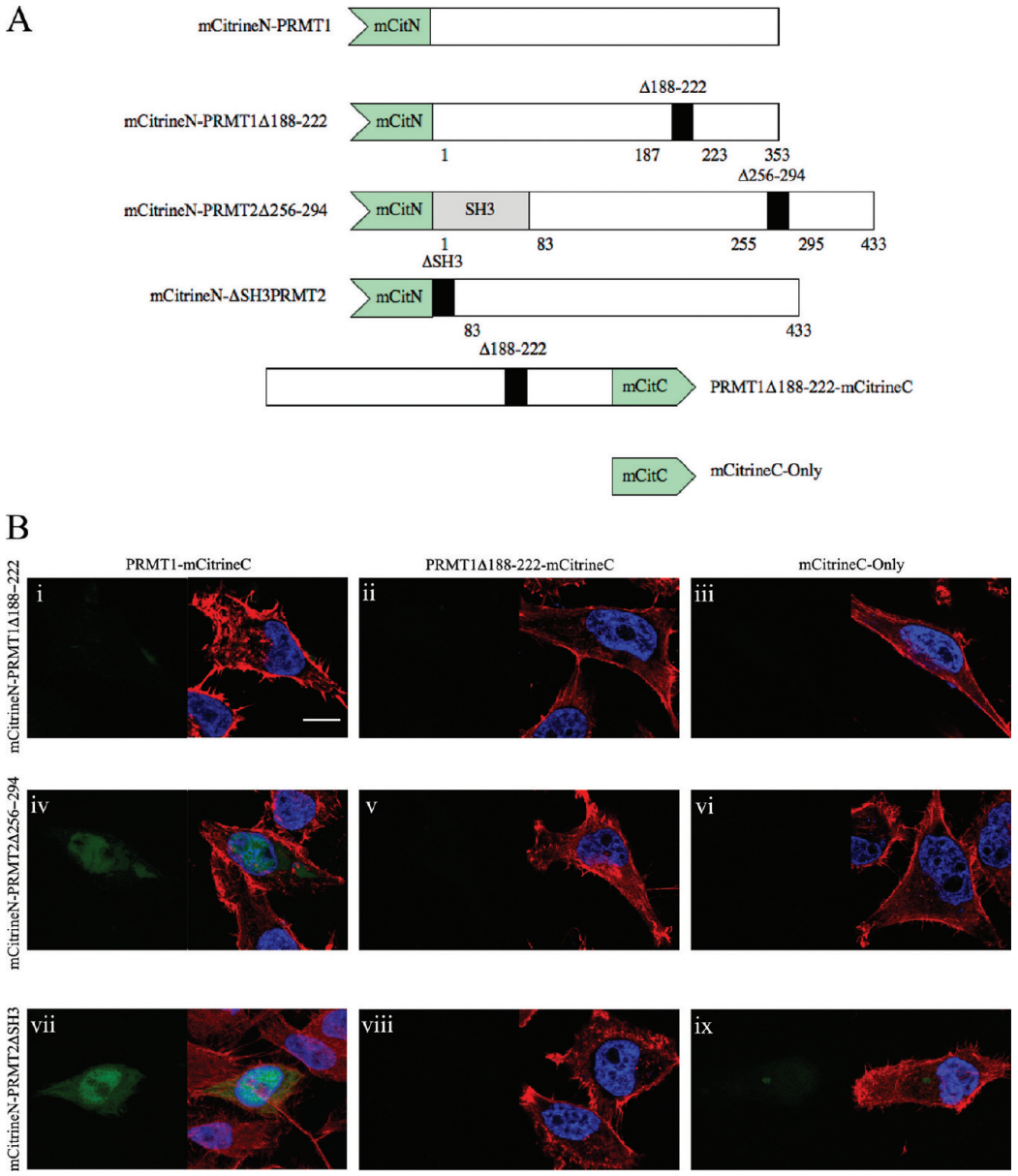

Figure 6. Effects of domain deletions in PRMT1 and -2 on BiFC complex formation. (A) Illustration of BiFC fusion proteins used in these experiments. (B) HeLa cells were cotransfected with the two constructs indicated in the columns and rows (representative images are shown). The left image of each row shows the formation of a BiFC complex. The right image of each row shows an overlay of BiFC (green), DAPI (blue), and fluorescence-labeled phalloidin (red). The scale bar is 10 μm.

similar to what occurred between both wild-type and mutant versions of PRMT2 and E153Q (Figure 7Bii,iv), and it is also consistent with the result for the PRMT1 and -2 co-immunoprecipitation performed in AdOx-treated cells for which no enrichment over background was observed (Figure 8A). In contrast, deletion of the PRMT2 SH3 domain did not affect its interaction with PRMT1 in the presence of AdOx as determined by BiFC (Figure 7Bvii) and co-immunoprecipitation (Figure 8B), providing additional evidence that the interaction between PRMT1 and -2 exhibits an SH3-dependent sensitivity to the state of methylation within the cell.

■ DISCUSSION

Activated PRMT1 via PRMT2 Association. The observation that PRMT1 is responsible for the bulk of total arginine methylation activity in cells[12,13] suggests two possibilities: (i) PRMT1 is the enzyme solely responsible for most of this activity, or (ii) most of the activity is dependent on PRMT1, but not to the exclusion of other PRMTs. In this study, we have identified a novel interaction between PRMT1 and -2 that provides evidence for the latter possibility in which PRMT1 shoulders most of the burden of transferring methyl groups as an activated complex with PRMT2.

Some studies have indicated that PRMT2 function in cells may be independent of any enzymatic activity, as in the cases in which PRMT2 in complex with the retinoblastoma gene product RB was shown to repress the transcriptional activity of E2F1[54] or in which it was demonstrated to promote apoptosis by retaining IκB-α in the nucleus to prevent NF-κB-dependent transcription.[55] The transcriptional coactivator functions of PRMT2, however, have been shown to require a functional

dx.doi.org/10.1021/bi200644c | Biochemistry 2011, 50, 8226–8240

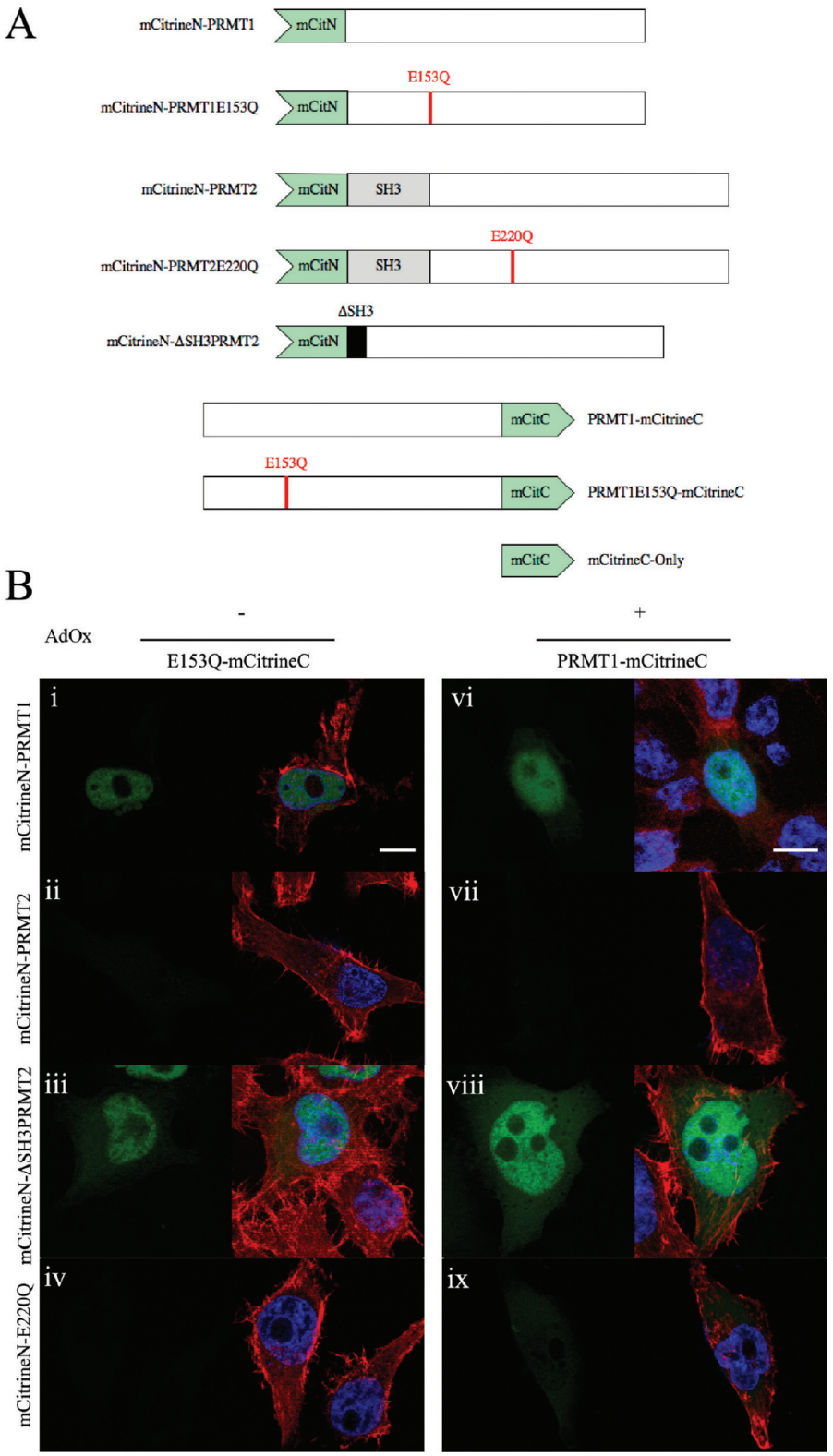

Figure 7. Effects of catalytically inactive PRMT1 and -2 on BiFC complex formation. (A) Illustration of BiFC fusion proteins used in these experiments. (B) HeLa cells treated with 20 μM AdOx or not treated were cotransfected with the two constructs indicated in the columns and rows (representative images are shown). The left image of each row shows the formation of a BiFC complex. The right image of each row shows an overlay of BiFC (green), DAPI (blue), and fluorescence-labeled phalloidin (red). The scale bar is 10 μm.

enzyme.[38,39,56] The ability of wild-type and catalytically inactive PRMT2 to potentiate PRMT1 activity in vitro supports an interaction between the two enzymes in which PRMT2 plays a scaffolding role for PRMT1. This role is further supported by the observed increase in methylarginine levels when PRMT2 as the wild type or inactive mutant was overexpressed in HeLa cells (Figure 3). The fact that the level of sDMA also increased along with those of aDMA and MMA implies that PRMT5

dx.doi.org/10.1021/bi200644c | *Biochemistry* 2011, 50, 8226–8240

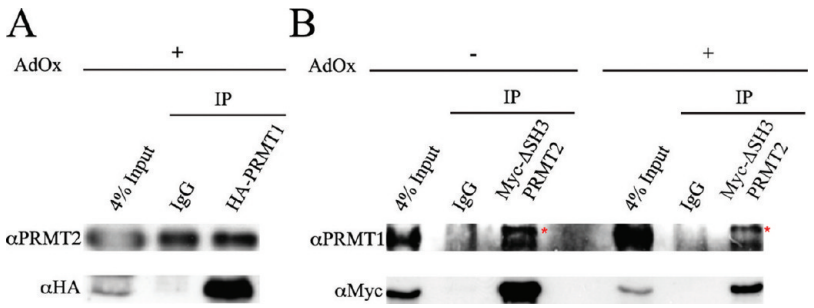

Figure 8. Co-immunoprecipitations of PRMT1 and PRMT2 in hypomethylated cells. (A) HA-PRMT1 was expressed in HeLa cells treated with 20 μM AdOx, and the cell lysate was immunoprecipitated with anti-HA antibody or with mouse IgG (negative control). Immunoprecipitates were immunoblotted with anti-PRMT2 (top) or anti-HA (bottom) antibodies. (B) c-Myc-ΔSH3PRMT2 was expressed in HeLa cells treated with 20 μM AdOx or not treated, and the cell lysate was immunoprecipitated with anti-Myc antibody or with mouse IgG (negative control). Immunoprecipitates were immunoblotted with anti-PRMT1 (top) or anti-Myc (bottom) antibodies. Nonspecific bands are labeled with red asterisks.

activity or expression may have been affected by the PRMT2-dependent activation of PRMT1.

The role that PRMT2 played in activating PRMT1 in cells appeared to result from its ability to serve as a subunit of a heteromeric complex as demonstrated in our in vitro studies. The apparent kinetic parameters for both combinations of PRMT1 with either E153Q or E220Q showed augmented V_{max} and k_{cat} values compared to those for PRMT1 alone (Table 1), and differences in K_M values for PRMT1 toward histone H4 and AdoMet. Similar changes in enzymatic activity and substrate specificity have been observed with PRMTs based on interactions with other proteins. For example, immediate-early/primary response gene products have been shown to modulate PRMT1 activity.[3] In addition, the substrate preference of PRMT5 can change depending on its interaction with either cofactor protein pICln or MEP50.[57] It follows then that other heteromeric complexes involving PRMT1 may form and exhibit altered activity and/or substrate specificity. In this study, we can only speculate that the increases in PRMT1 activity with excess PRMT1 or PRMT2 subunits (Figures 1 and 2) can be attributed to the formation of higher-order oligomeric structures, perhaps resembling complexes observed for crystal structures of PRMT1 and its yeast homologue.[28,29]

PRMT1 and -2 Associations in Cells. The association between endogenous PRMT1 or -2 and HA-tagged PRMT1 or -2 from HeLa cells was demonstrated by Western blot analysis after co-immunoprecipitation (Figure 4B,C). This interaction can barely be seen in a Western blot from another study in which GFP-PRMT1 was co-immunoprecipitated from cells with GFP-PRMT2 using anti-PRMT2 antibodies,[27] indicating that the interaction between PRMT1 and -2 may be transient with a binding affinity weaker than what has been observed for PRMT1 and -6 homodimers.[42] The use of BiFC in this instance has provided for an alternative means of capturing direct partnering between PRMT1 subunits, as well as between PRMT1 and -2 subunits. Because deletion of the SH3 domain on PRMT2 did not eliminate complex formation, we were able to rule it out as a possible binding module that is directly responsible for the PRMT1−PRMT2 interaction (Figure 6Bvii). Despite the fact that two PRMT2 subunits did not form a BiFC complex (Figure 5Bv), we were able to co-immunoprecipitate endogenous PRMT2 with HA-tagged PRMT2 (Figure S9A of the Supporting Information). Indeed, Fackelmayer and co-workers as well as our own group have previously reported evidence of PRMT2 dimerization.[4,27]

In this study, we used only one of the seven PRMT1 splice variants, PRMT1v1.[58] Neither PRMT1v1 nor PRMT2 contains nuclear localization signals within their sequences, but it is possible that the observed complexes may initially associate in either cytoplasmic or nuclear compartments and become trapped in the nucleus (Figure 5Bi,iv). We are aware that differences in the efficiency of fixation for organelles from experiment to experiment have been reported as a source of potential artifacts in the localization of soluble proteins.[59] PRMT1, PRMT2, and ΔSH3PRMT2 expressed individually in HeLa cells as fusions with full-length mCitrine were localized in both cellular compartments consistent with previous results,[8] and this pattern was not altered when cells were coexpressed mCitrine-PRMT1 and mCitrine-PRMT2 (Figure S12 of the Supporting Information). Fackelmayer and co-workers have demonstrated that PRMT subcellular localization can be different depending on cell type.[27] Thus, it is unclear if the mostly nuclear localization of BiFC complexes for PRMT1 and -2 observed in HeLa cells is representative of where they may reside in other cell lines. Additionally, PRMT1 isoforms characterized by Côté and co-workers that exhibited distinct subcellular localizations, particularly the PRMT1v2 isoform bearing a nuclear export signal that localizes it to the cytoplasm,[58] may have an impact on where PRMT1 interactions present as BiFC complexes in cells. Whether PRMT2 interacts with all seven PRMT1 isoforms is currently under investigation.

Methylation-Dependent Mediation of Formation of the PRMT1−PRMT2 Complex. The inactive PRMT1 E153Q mutant was previously shown to exhibit oligomeric structure and AdoMet binding ability similar to those of the wild-type enzyme.[28] Using this mutation in our BiFC assay confirmed that PRMT1 self-association is independent of its catalytic activity (Figure 7Bi and Figure S7i,ii of the Supporting Information). AdOx treatment to reduce the methylation potential of the cell also did not impact PRMT1 pairing (Figure 7Bv), which is consistent with the finding from Fackelmayer and co-workers that a PRMT1−GFP fusion protein maintained a presence in a high-molecular mass complex with or without AdOx treatment.[27] In contrast, the interaction between PRMT1 and -2 was solely dependent on PRMT1 activity as determined either by inactive mutant E153Q (Figure 7Bii,iv and Figure S7iii of the Supporting Information) or by AdOx treatment (Figures 7Bvi,viii and 8A). Unlike the effect on PRMT1-GFP with AdOx treatment, the mobility of the PRMT2-GFP fusion protein was reduced in cells, indicating, as the authors point out, that PRMTs responded differently to the accumulation of

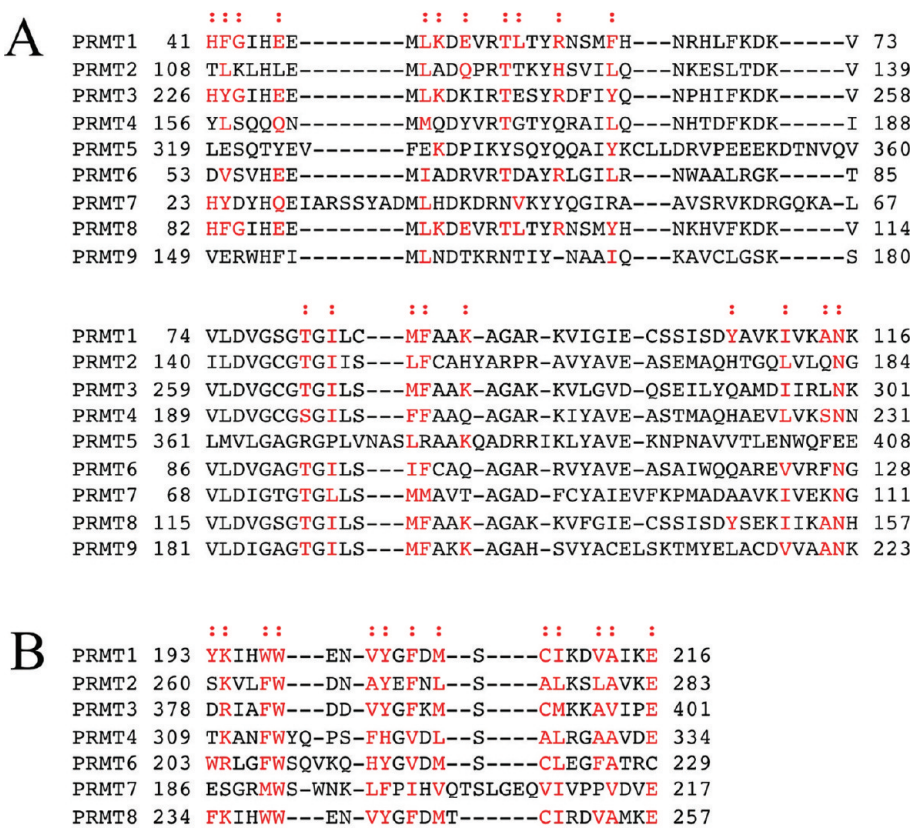

Figure 9. Sequence alignment of residues at the PRMT dimer interface. Sequences for human PRMTs that may be involved in dimer contacts were aligned using protein-protein BLAST (NCBI). In some instances, sequences could not be aligned because of insufficient similarity and are not included. Residues reported in PRMT crystal structures to make direct contacts at the dimer interface between sequences in panels A and B are indicated with a colon, and dimer residues[28−32] similar to the PRMT1 sequence are highlighted in red.

unmethylated substrates.[27] In this study, we have found that the interaction between PRMT1 and -2 appeared to be sensitive to the methylation state of one or more unknown substrates, which were presumably modified by PRMT1 on the basis of evidence presented above.

A deletion of the SH3 domain from PRMT2 had restored formation of the PRMT1−PRMT2 complex regardless of PRMT1 inactivity or AdOx treatment. These results imply that the recognition of SH3 domain ligands, possibly as methylated substrates, has an impact on assembly of the PRMT1−PRMT2 complex. We propose that the SH3 domain or another mediator bearing a proline-rich sequence to which the SH3 domain can bind controls the formation of the complete complex.

A handful of PRMT2 SH3 domain ligands that are also methyl acceptors have already been identified. The first ligand shown to bind to PRMT2 through its SH3 domain was the arginine methyltransferase substrate hnRNP E1B-AP5, an interaction that was initially found via a yeast two-hybrid screen and demonstrated using co-immunoprecipitation and in situ immunofluorescence.[60] In a protein domain microarray, an immobilized GST-SH3 (PRMT2) was able to tightly bind to the core small nuclear ribonucleoprotein SmB′ and Sam68,[61] both of which contain polyproline stretches that are known recognition sequences for SH3 domain binding.[62] Indeed, the proline-rich N-terminus of PRMT8 was also shown to bind to the PRMT2 SH3 domain.[52] Recently, a yeast two-hybrid screen identified an interaction between the PRMT2 SH3 domain and mammalian cleavage factor I (CF I_m59), which is an hnRNP and PRMT substrate that contains polyproline sequences.[57]

Given the importance of the SH3 domain in mediating interactions for PRMT2, it is conceivable that the methylation state of specific substrates affects the interaction between PRMT1 and -2. The association of PRMT1 with its substrates, such as hnRNP U[63] and Sam68,[64] suggests that these RNA-binding proteins are ideal candidates for serving an additional scaffolding role in mediating the interaction between PRMT1 and -2. Sam68 has been shown to bridge the interaction between PRMT1 and the *Mixed Lineage Leukemia* oncogenic complex (MLL-EEN) as a required scaffold for hematopoietic cell transformation, and mediating this interaction is the SH3 domain from MLL-EEN binding to polyproline sequences in Sam68.[65] Because the SH3 domain is a unique feature of PRMT2 within its enzyme family, the identification of its endogenous ligands will aid in our understanding of its role in PRMT2 interactions.

Conclusion. In this study, we have presented evidence that PRMT1 and -2 interact in vitro and in cells, and that PRMT1 activity increases as a result. A kinetic analysis of PRMT1 with a catalytically inactive E153Q or E220Q mutant revealed that these subunits increased V_{max} and k_{cat} for PRMT1 while differentially affecting AdoMet and histone H4 K_M values. These data suggest that the PRMT1 binding partner, in this case PRMT2, can influence the substrate specificity of the resulting complex. A sequence alignment of regions purported to be involved in dimer formation among human PRMT family members indicates that dimer-contacting residues are conserved (Figure 9). Therefore, it is interesting to speculate that different heteromeric PRMT combinations could form,

resulting in a host of distinct substrate preferences that enhance the diversity of PRMT functions on the cellular level.

■ ASSOCIATED CONTENT

Ⓢ Supporting Information

Supporting experimental details, Tables S1 and S2, and Figures S1−S12. This material is available free of charge via the Internet at http://pubs.acs.org.

■ AUTHOR INFORMATION

Corresponding Author

*Telephone: (604) 822-7146. Fax; (604) 822-3035. E-mail: afrankel@mail.ubc.ca.

Funding

This work was supported by Canadian Institutes of Health Research Grant MOP 79271, the Canada Research Chairs program (A.F.), and a four-year University Graduate Fellowship Award from The University of British Columbia (D.T.).

■ ACKNOWLEDGMENTS

We thank Drs. Ujendra Kumar, Rishi Somvanshi, and Padmesh Rajput for advice, mammalian expression vectors, and use of their upright fluorescence microscope. We also thank Dr. Karolin Luger (Colorado State University) for providing us with an expression plasmid for histone H4. We acknowledge the Bioimaging Facility and the Faculty of Pharmaceutical Sciences Mass Spectrometry Facility at The University of British Columbia for their expertise and help with this project.

■ ABBREVIATIONS

aDMA	asymmetric ω-N^G,N^G-dimethylarginine
AdoMet	*S*-adenosyl-L-methionine
AdOx	periodate-oxidized adenosine
BiFC	bimolecular fluorescence complementation
BSA	bovine serum albumin
CARM1	coactivator-associated arginine methyltransferase
DAPI	2-(4-carbamimidoylphenyl)-1*H*-indole-6-carboximidamide
GFP	green fluorescent protein
GST	glutathione *S*-transferase
HA	hemagglutinin
hnRNP	heterogeneous nuclear ribonucleoprotein
mCitrineC	amino acid residues 174−239 of monomeric citrine
mCitrineN	amino acid residues 1−173 of monomeric citrine
MMA	ω-N^G-monomethylarginine
NR	nuclear receptor
PRMT	protein arginine *N*-methyltransferase
sDMA	symmetric ω-N^G,N^G-dimethylarginine
SH3	Src homology 3.

■ REFERENCES

(1) Bedford, M. T., and Clarke, S. G. (2009) Protein arginine methylation in mammals: Who, what, and why. *Mol. Cell 33*, 1−13.

(2) Bedford, M. T. (2007) Arginine methylation at a glance. *J. Cell Sci. 120*, 4243−4246.

(3) Lin, W. J., Gary, J. D., Yang, M. C., Clarke, S., and Herschman, H. R. (1996) The mammalian immediate-early TIS21 protein and the leukemia-associated BTG1 protein interact with a protein-arginine *N*-methyltransferase. *J. Biol. Chem. 271*, 15034−15044.

(4) Lakowski, T. M., and Frankel, A. (2009) Kinetic analysis of human protein arginine *N*-methyltransferase 2: Formation of monomethyl- and asymmetric dimethyl-arginine residues on histone H4. *Biochem. J. 421*, 253−261.

(5) Tang, J., Gary, J. D., Clarke, S., and Herschman, H. R. (1998) PRMT 3, a type I protein arginine *N*-methyltransferase that differs from PRMT1 in its oligomerization, subcellular localization, substrate specificity, and regulation. *J. Biol. Chem. 273*, 16935−16945.

(6) Chen, D., Ma, H., Hong, H., Koh, S. S., Huang, S. M., Schurter, B. T., Aswad, D. W., and Stallcup, M. R. (1999) Regulation of transcription by a protein methyltransferase. *Science 284*, 2174−2177.

(7) Schurter, B. T., Koh, S. S., Chen, D., Bunick, G. J., Harp, J. M., Hanson, B. L., Henschen-Edman, A., Mackay, D. R., Stallcup, M. R., and Aswad, D. W. (2001) Methylation of histone H3 by coactivator-associated arginine methyltransferase 1. *Biochemistry 40*, 5747−5756.

(8) Frankel, A., Yadav, N., Lee, J., Branscombe, T. L., Clarke, S., and Bedford, M. T. (2002) The novel human protein arginine *N*-methyltransferase PRMT6 is a nuclear enzyme displaying unique substrate specificity. *J. Biol. Chem. 277*, 3537−3543.

(9) Lee, J., Sayegh, J., Daniel, J., Clarke, S., and Bedford, M. T. (2005) PRMT8, a new membrane-bound tissue-specific member of the protein arginine methyltransferase family. *J. Biol. Chem. 280*, 32890−32896.

(10) Branscombe, T. L., Frankel, A., Lee, J. H., Cook, J. R., Yang, Z., Pestka, S., and Clarke, S. (2001) PRMT5 (Janus kinase-binding protein 1) catalyzes the formation of symmetric dimethylarginine residues in proteins. *J. Biol. Chem. 276*, 32971−32976.

(11) Miranda, T. B., Miranda, M., Frankel, A., and Clarke, S. (2004) PRMT7 is a member of the protein arginine methyltransferase family with a distinct substrate specificity. *J. Biol. Chem. 279*, 22902−22907.

(12) Tang, J., Kao, P. N., and Herschman, H. R. (2000) Protein-arginine methyltransferase I, the predominant protein-arginine methyltransferase in cells, interacts with and is regulated by interleukin enhancer-binding factor 3. *J. Biol. Chem. 275*, 19866−19876.

(13) Pawlak, M. R., Scherer, C. A., Chen, J., Roshon, M. J., and Ruley, H. E. (2000) Arginine *N*-methyltransferase 1 is required for early postimplantation mouse development, but cells deficient in the enzyme are viable. *Mol. Cell. Biol. 20*, 4859−4869.

(14) Barrero, M. J., and Malik, S. (2006) Two functional modes of a nuclear receptor-recruited arginine methyltransferase in transcriptional activation. *Mol. Cell 24*, 233−243.

(15) Le Romancer, M., Treilleux, I., Leconte, N., Robin-Lespinasse, Y., Sentis, S., Bouchekioua-Bouzaghou, K., Goddard, S., Gobert-Gosse, S., and Corbo, L. (2008) Regulation of estrogen rapid signaling through arginine methylation by PRMT1. *Mol. Cell 31*, 212−221.

(16) Wang, H., Huang, Z. Q., Xia, L., Feng, Q., Erdjument-Bromage, H., Strahl, B. D., Briggs, S. D., Allis, C. D., Wong, J., Tempst, P., and Zhang, Y. (2001) Methylation of histone H4 at arginine 3 facilitating transcriptional activation by nuclear hormone receptor. *Science 293*, 853−857.

(17) Strahl, B. D., Briggs, S. D., Brame, C. J., Caldwell, J. A., Koh, S. S., Ma, H., Cook, R. G., Shabanowitz, J., Hunt, D. F., Stallcup, M. R., and Allis, C. D. (2001) Methylation of histone H4 at arginine 3 occurs in vivo and is mediated by the nuclear receptor coactivator PRMT1. *Curr. Biol. 11*, 996−1000.

(18) Chiou, Y. Y., Lin, W. J., Fu, S. L., and Lin, C. H. (2007) Direct mass-spectrometric identification of Arg296 and Arg299 as the methylation sites of hnRNP K protein for methyltransferase PRMT1. *Protein J. 26*, 87−93.

(19) Ostareck-Lederer, A., Ostareck, D. H., Rucknagel, K. P., Schierhorn, A., Moritz, B., Huttelmaier, S., Flach, N., Handoko, L., and Wahle, E. (2006) Asymmetric arginine dimethylation of heterogeneous nuclear ribonucleoprotein K by protein-arginine methyltransferase 1 inhibits its interaction with c-Src. *J. Biol. Chem. 281*, 11115−11125.

(20) Liu, Q., and Dreyfuss, G. (1995) In vivo and in vitro arginine methylation of RNA-binding proteins. *Mol. Cell. Biol. 15*, 2800−2808.

(21) Koh, S. S., Chen, D., Lee, Y. H., and Stallcup, M. R. (2001) Synergistic enhancement of nuclear receptor function by p160 coactivators and two coactivators with protein methyltransferase activities. *J. Biol. Chem. 276*, 1089−1098.

(22) An, W., Kim, J., and Roeder, R. G. (2004) Ordered cooperative functions of PRMT1, p300, and CARM1 in transcriptional activation by p53. *Cell 117*, 735−748.
(23) Kleinschmidt, M. A., Streubel, G., Samans, B., Krause, M., and Bauer, U. M. (2008) The protein arginine methyltransferases CARM1 and PRMT1 cooperate in gene regulation. *Nucleic Acids Res. 36*, 3202−3213.
(24) Hassa, P. O., Covic, M., Bedford, M. T., and Hottiger, M. O. (2008) Protein arginine methyltransferase 1 coactivates NF-κB-dependent gene expression synergistically with CARM1 and PARP1. *J. Mol. Biol. 377*, 668−678.
(25) El-Andaloussi, N., Valovka, T., Toueille, M., Steinacher, R., Focke, F., Gehrig, P., Covic, M., Hassa, P. O., Schar, P., Hubscher, U., and Hottiger, M. O. (2006) Arginine methylation regulates DNA polymerase β. *Mol. Cell 22*, 51−62.
(26) El-Andaloussi, N., Valovka, T., Toueille, M., Hassa, P. O., Gehrig, P., Covic, M., Hubscher, U., and Hottiger, M. O. (2007) Methylation of DNA polymerase β by protein arginine methyltransferase 1 regulates its binding to proliferating cell nuclear antigen. *FASEB J. 21*, 26−34.
(27) Herrmann, F., Pably, P., Eckerich, C., Bedford, M. T., and Fackelmayer, F. O. (2009) Human protein arginine methyltransferases in vivo: Distinct properties of eight canonical members of the PRMT family. *J. Cell Sci. 122*, 667−677.
(28) Zhang, X., and Cheng, X. (2003) Structure of the predominant protein arginine methyltransferase PRMT1 and analysis of its binding to substrate peptides. *Structure 11*, 509−520.
(29) Weiss, V. H., McBride, A. E., Soriano, M. A., Filman, D. J., Silver, P. A., and Hogle, J. M. (2000) The structure and oligomerization of the yeast arginine methyltransferase, Hmt1. *Nat. Struct. Biol. 7*, 1165−1171.
(30) Zhang, X., Zhou, L., and Cheng, X. (2000) Crystal structure of the conserved core of protein arginine methyltransferase PRMT3. *EMBO J. 19*, 3509−3519.
(31) Yue, W. W., Hassler, M., Roe, S. M., Thompson-Vale, V., and Pearl, L. H. (2007) Insights into histone code syntax from structural and biochemical studies of CARM1 methyltransferase. *EMBO J. 26*, 4402−4412.
(32) Troffer-Charlier, N., Cura, V., Hassenboehler, P., Moras, D., and Cavarelli, J. (2007) Functional insights from structures of coactivator-associated arginine methyltransferase 1 domains. *EMBO J. 26*, 4391−4401.
(33) Pollack, B. P., Kotenko, S. V., He, W., Izotova, L. S., Barnoski, B. L., and Pestka, S. (1999) The human homologue of the yeast proteins Skb1 and Hsl7p interacts with Jak kinases and contains protein methyltransferase activity. *J. Biol. Chem. 274*, 31531−31542.
(34) Rho, J., Choi, S., Seong, Y. R., Cho, W. K., Kim, S. H., and Im, D. S. (2001) Prmt5, which forms distinct homo-oligomers, is a member of the protein-arginine methyltransferase family. *J. Biol. Chem. 276*, 11393−11401.
(35) Higashimoto, K., Kuhn, P., Desai, D., Cheng, X., and Xu, W. (2007) Phosphorylation-mediated inactivation of coactivator-associated arginine methyltransferase 1. *Proc. Natl. Acad. Sci. U.S.A. 104*, 12318−12323.
(36) Katsanis, N., Yaspo, M. L., and Fisher, E. M. (1997) Identification and mapping of a novel human gene, HRMT1L1, homologous to the rat protein arginine *N*-methyltransferase 1 (PRMT1) gene. *Mamm. Genome 8*, 526−529.
(37) Scott, H. S., Antonarakis, S. E., Lalioti, M. D., Rossier, C., Silver, P. A., and Henry, M. F. (1998) Identification and characterization of two putative human arginine methyltransferases (HRMT1L1 and HRMT1L2). *Genomics 48*, 330−340.
(38) Meyer, R., Wolf, S. S., and Obendorf, M. (2007) PRMT2, a member of the protein arginine methyltransferase family, is a coactivator of the androgen receptor. *J. Steroid Biochem. Mol. Biol. 107*, 1−14.
(39) Qi, C., Chang, J., Zhu, Y., Yeldandi, A. V., Rao, S. M., and Zhu, Y. J. (2002) Identification of protein arginine methyltransferase 2 as a coactivator for estrogen receptor α. *J. Biol. Chem. 277*, 28624−28630.
(40) Ghosh, I., Hamilton, A. D., and Regan, L. (2000) Antiparallel Leucine Zipper-Directed Protein Reassembly: Application to the Green Fluorescent Protein. *J. Am. Chem. Soc. 122*, 5658−5659.
(41) Hu, C. D., Chinenov, Y., and Kerppola, T. K. (2002) Visualization of interactions among bZIP and Rel family proteins in living cells using bimolecular fluorescence complementation. *Mol. Cell 9*, 789−798.
(42) Thomas, D., Lakowski, T. M., Pak, M. L., Kim, J. J., and Frankel, A. (2010) Förster resonance energy transfer measurements of cofactor-dependent effects on protein arginine *N*-methyltransferase homodimerization. *Protein Sci. 19*, 2141−2151.
(43) Tilsner, J., Linnik, O., Christensen, N. M., Bell, K., Roberts, I. M., Lacomme, C., and Oparka, K. J. (2009) Live-cell imaging of viral RNA genomes using a Pumilio-based reporter. *Plant J. 57*, 758−770.
(44) Luger, K., Rechsteiner, T. J., Flaus, A. J., Waye, M. M., and Richmond, T. J. (1997) Characterization of nucleosome core particles containing histone proteins made in bacteria. *J. Mol. Biol. 272*, 301−311.
(45) Teerlink, T., Nijveldt, R. J., de Jong, S., and van Leeuwen, P. A. (2002) Determination of arginine, asymmetric dimethylarginine, and symmetric dimethylarginine in human plasma and other biological samples by high-performance liquid chromatography. *Anal. Biochem. 303*, 131−137.
(46) Magliery, T. J., Wilson, C. G., Pan, W., Mishler, D., Ghosh, I., Hamilton, A. D., and Regan, L. (2005) Detecting protein-protein interactions with a green fluorescent protein fragment reassembly trap: Scope and mechanism. *J. Am. Chem. Soc. 127*, 146−157.
(47) Kerppola, T.K. (2006) Visualization of molecular interactions by fluorescence complementation. *Nat. Rev. Mol. Cell Biol. 7*, 449−456.
(48) Kerppola, T. K. (2009) Visualization of molecular interactions using bimolecular fluorescence complementation analysis: Characteristics of protein fragment complementation. *Chem. Soc. Rev. 38*, 2876−2886.
(49) Morell, M., Espargaro, A., Aviles, F. X., and Ventura, S. (2007) Detection of transient protein-protein interactions by bimolecular fluorescence complementation: The Abl-SH3 case. *Proteomics 7*, 1023−1036.
(50) Vidi, P. A., and Watts, V. J. (2009) Fluorescent and bioluminescent protein-fragment complementation assays in the study of G protein-coupled receptor oligomerization and signaling. *Mol. Pharmacol. 75*, 733−739.
(51) Griesbeck, O., Baird, G. S., Campbell, R. E., Zacharias, D. A., and Tsien, R. Y. (2001) Reducing the environmental sensitivity of yellow fluorescent protein. Mechanism and applications. *J. Biol. Chem. 276*, 29188−29194.
(52) Sayegh, J., Webb, K., Cheng, D., Bedford, M. T., and Clarke, S. G. (2007) Regulation of protein arginine methyltransferase 8 (PRMT8) activity by its N-terminal domain. *J. Biol. Chem. 282*, 36444−36453.
(53) Bartel, R. L., and Borchardt, R. T. (1984) Effects of adenosine dialdehyde on *S*-adenosylhomocysteine hydrolase and *S*-adenosylmethionine-dependent transmethylations in mouse L929 cells. *Mol. Pharmacol. 25*, 418−424.
(54) Yoshimoto, T., Boehm, M., Olive, M., Crook, M. F., San, H., Langenickel, T., and Nabel, E. G. (2006) The arginine methyltransferase PRMT2 binds RB and regulates E2F function. *Exp. Cell Res. 312*, 2040−2053.
(55) Ganesh, L., Yoshimoto, T., Moorthy, N. C., Akahata, W., Boehm, M., Nabel, E. G., and Nabel, G. J. (2006) Protein methyltransferase 2 inhibits NF-κB function and promotes apoptosis. *Mol. Cell. Biol. 26*, 3864−3874.
(56) Blythe, S. A., Cha, S. W., Tadjuidje, E., Heasman, J., and Klein, P. S. (2010) β-Catenin primes organizer gene expression by recruiting a histone H3 arginine 8 methyltransferase, Prmt2. *Dev. Cell 19*, 220−231.
(57) Martin, G., Ostareck-Lederer, A., Chari, A., Neuenkirchen, N., Dettwiler, S., Blank, D., Ruegsegger, U., Fischer, U., and Keller, W. (2010) Arginine methylation in subunits of mammalian pre-mRNA cleavage factor I. *RNA 16*, 1646−1659.

(58) Goulet, I., Gauvin, G., Boisvenue, S., and Cote, J. (2007) Alternative splicing yields protein arginine methyltransferase 1 isoforms with distinct activity, substrate specificity, and subcellular localization. *J. Biol. Chem. 282*, 33009−33021.
(59) Herrmann, F., Lee, J., Bedford, M. T., and Fackelmayer, F. O. (2005) Dynamics of human protein arginine methyltransferase 1(PRMT1) in vivo. *J. Biol. Chem. 280*, 38005−38010.
(60) Kzhyshkowska, J., Schutt, H., Liss, M., Kremmer, E., Stauber, R., Wolf, H., and Dobner, T. (2001) Heterogeneous nuclear ribonucleoprotein E1B-AP5 is methylated in its Arg-Gly-Gly (RGG) box and interacts with human arginine methyltransferase HRMT1L1. *Biochem. J. 358*, 305−314.
(61) Espejo, A., Cote, J., Bednarek, A., Richard, S., and Bedford, M. T. (2002) A protein-domain microarray identifies novel protein-protein interactions. *Biochem. J. 367*, 697−702.
(62) Ren, R., Mayer, B. J., Cicchetti, P., and Baltimore, D. (1993) Identification of a ten-amino acid proline-rich SH3 binding site. *Science 259*, 1157−1161.
(63) Herrmann, F., Bossert, M., Schwander, A., Akgun, E., and Fackelmayer, F. O. (2004) Arginine methylation of scaffold attachment factor A by heterogeneous nuclear ribonucleoprotein particle-associated PRMT1. *J. Biol. Chem. 279*, 48774−48779.
(64) Cote, J., Boisvert, F. M., Boulanger, M. C., Bedford, M. T., and Richard, S. (2003) Sam68 RNA binding protein is an in vivo substrate for protein arginine N-methyltransferase 1. *Mol. Biol. Cell 14*, 274−287.
(65) Cheung, N., Chan, L. C., Thompson, A., Cleary, M. L., and So, C. W. (2007) Protein arginine-methyltransferase-dependent oncogenesis. *Nat. Cell Biol. 9*, 1208−1215.